IEEE Access
Multidisciplinary | Rapid Review | Open Access Journal

Received February 6, 2019, accepted February 24, 2019, date of publication March 11, 2019, date of current version March 25, 2019.

Digital Object Identifier 10.1109/ACCESS.2019.2902466

Volumetric Invisibility Cloaks Design Through Spectral Coverage Optimization

ROBERTA PALMERI AND TOMMASO ISERNIA, (Senior Member, IEEE)
Dipartimento di Ingegneria dell'Informazione, delle Infrastrutture e dell'Energia Sostenibile, Università degli Studi Mediterranea di Reggio Calabria, 89124 Reggio Calabria, Italy

Corresponding author: Roberta Palmeri (roberta.palmeri@unirc.it)

ABSTRACT A novel approach to the design of cloaking devices is presented which takes inspiration from the Fourier diffraction theorem. In particular, we first put on a common basis different linear approximations of the scattering equations. Then, a very simple procedure to get invisibility (under the given approximation at hand) is proposed. The approach is assessed through numerical examples concerning 3-D non-canonical objects.

INDEX TERMS Fourier diffraction theorem, inverse design, linear approximations, scattering.

I. INTRODUCTION

In 2005, Alù and Engheta [1] were the pioneers of the concept of volumetric cloaks with the well-known *scattering cancellation* (SC) theory. As such, in [1] they demonstrated the actual possibility of making invisible a small dielectric object by covering it with a volumetric material (*cloak*) able to balance the polarization of the dielectric. To this aim, cloaks could present exotic material properties, namely they could be *artificial materials* or *metamaterials*.

Starting from this new concept, a number of papers concerning the applicability of SC in different scenarios have been published [2]–[8].

In the same period, the Transformation Optics (TO) theory was also developed [9], which is based on proper spatial coordinates transformation. For the specific invisibility problem at hand, TO allows the bending of the waves just outside the region occupied by the dielectric object, so that no interaction is possible amongst the incident fields and the object to be hidden. Differently from the SC, in this case the cloak is object-independent, but the arising materials properties are inhomogeneous and strongly anisotropic. Many applications of the TO framework can be found for both cloaking [10], [11] and radiation [12], [13] problems.

Recently, the framework of inverse scattering problems, that is widely applied for diagnosis purposes, has been explored as a powerful synthesis tool for both antennas [14]–[18] and cloaking problems [19], [20]. However, design approaches based on the solution of a generic inverse scattering problem have to face non-linearity and ill-posedness (in the Hadamard's sense) [21] issues. As a consequence, just a few results have been presented in the literature based on inverse scattering and, because of the computational burden, they are indeed limited to 2-D geometries. Moreover, because of non-linearity, one is not able to understand actual limitations of the approach.

Based on these circumstances, as well as on the circumstance that the popular SC technique also works under some hypotheses on the object to be hidden, in this contribution we propose an alternative and very simple approach to design volumetric invisibility cloaks for dielectric objects that applies to both 2-D and 3-D geometries under a number of different linear approximations.

In particular, by generalizing a result which is well-known under the Born approximation (BA), we show that also for the Contrast Source Extended Born (CS-EB) [22] and [23] and Strong Permittivity Fluctuation (SPF) [24], [25] approximations (and using plane wave incidences and far field measurements) the scattered field can be related to the Fourier transform of the unknown function embedding the characteristics of the target to be hidden. More in detail, the knowledge of the scattered field for all incidence-observation directions is equivalent to the knowledge of the Fourier transform of the unknown in a circle (sphere) of radius $2k_b$ [26]. Hence, a very simple strategy to get invisibility can be developed by a proper Fourier-analysis-based engineering of the cloak. Notably, the approach keeps valid also in case transmitting and receiving antennas are not located in the far field of the

The associate editor coordinating the review of this manuscript and approving it for publication was Shah Nawaz Burokur.

TABLE 1. Summary of approximated models.

	Involved quantities	*State and Data exact Equations*	*Hypotheses and corresponding approximation*	*Unknown and approximated model*
EFIE and Born approximation (BA)	$\chi(\underline{r})$	$\underline{E} = \underline{E}_i + \boldsymbol{A_i}[\chi\underline{E}]$ $\underline{E}_s = \boldsymbol{A_e}[\chi\underline{E}]$	$\|\boldsymbol{A_i}\chi\| \ll 1$ $\underline{E}(\underline{r}) = \underline{E}_i(\underline{r})$	$\chi(\underline{r})$ $\underline{E} = \underline{E}_i$ $\underline{E}_s = \boldsymbol{A_e}[\chi\underline{E}_i]$
CS-EB formulation and corresponding approximation (CS-EBA)	$p(\underline{r}) = \frac{\chi(\underline{r})}{1-\chi(\underline{r})f_{\mathrm{Vm}}(\underline{r})}$ $f_{\mathrm{Vm}}(\underline{r}) = k_b^2\int_V \mathbf{G}(\underline{r}-\underline{r}')\,d\underline{r}'$	$\underline{W} = p\underline{E}_i + p\boldsymbol{A_{iMOD}}[\underline{W}]$ $\underline{E}_s = \boldsymbol{A_e}[\underline{W}]$	$\|p\boldsymbol{A_{iMOD}}\| \ll 1$ $\underline{W}(\underline{r}) = p(\underline{r})\underline{E}_i(\underline{r})$	$p(\underline{r})$ $\underline{W} = p\underline{E}_i$ $\underline{E}_s = \boldsymbol{A_e}[p\underline{E}_i]$
SPF formulation and corresponding approximation (SPFA)	$q(\underline{r}) = \frac{\chi(\underline{r})}{1+L\chi(\underline{r})}$ $L = \begin{cases}\frac{1}{2}\ (2D problems)\\ \frac{1}{3}\ (3D problems)\end{cases}$	$\underline{F} = \underline{E}_i + \boldsymbol{A_{iSPF}}[q\underline{F}]$ $\underline{E}_s = \boldsymbol{A_e}[q\underline{F}]$	$\|\boldsymbol{A_{iSPF}}q\| \ll 1$ $\underline{F}(\underline{r}) = \underline{E}_i(\underline{r})$	$q(\underline{r})$ $\underline{F} = \underline{E}_i$ $\underline{E}_s = \boldsymbol{A_e}[q\underline{E}_i]$

object as long as reactive fields of the antennas do not come into play.

The remainder of the paper is organized as follows. In Section II, mathematical formulations of the inverse scattering problem are briefly recalled and a number of linear approximations are derived. The novel design strategy is presented in Section III and then assessed through numerical examples in Section IV. Finally, conclusions are drawn. An Appendix section is devoted to the implementation of the optimization algorithm involved in the design problem.

II. FORMULATION OF THE INVERSE SCATTERING PROBLEM

To mathematically describe the scattering phenomenon, let us briefly recall the usual *electric field integral equation* (EFIE) based formulation for the case of isotropic and non-magnetic penetrable scatterers [27].

Let $V \subseteq \mathbb{R}^3$ be a volume enclosing a volumetric object characterized by a complex permittivity $\varepsilon_s(\underline{r})$ and embedded in a homogeneous background of permittivity ε_b. The EFIE reads as (the time factor $\exp(j\omega t)$ has been omitted):

$$\underline{E}(\underline{r}) = \underline{E}_i(\underline{r}) + \underline{E}_s(\underline{r}) \tag{1.a}$$

$$\underline{E}_s(\underline{r}) = k_b^2\int_V \mathbf{G}(\underline{r},\underline{r}')\,\chi(\underline{r}')\,\underline{E}(\underline{r}')\,d\underline{r}' \tag{1.b}$$

wherein $\underline{E}_s$ is the scattered field generated by the interaction with an incident field $\underline{E}_i$, while $\underline{E}$ is the arising induced total field in V; $k_b^2 = \omega^2\varepsilon_b\mu_0$ is the background wavenumber, μ_0 being the free-space magnetic permeability, $\mathbf{G}$ denotes the dyadic Green's function for a homogeneous space [27], and $\chi(\underline{r}) = \frac{\varepsilon_s(\underline{r})}{\varepsilon_b} - 1$ is the contrast function describing the electromagnetic parameters of the scatterer with respect to the background.

Notably, the state equation (1.a) and the data equation (1.b) can be written in an operator form as:

$$\underline{E} = \underline{E}_i + \boldsymbol{A_i}[\chi\underline{E}] \tag{1.c}$$

$$\underline{E}_s = \boldsymbol{A_e}[\chi\underline{E}] \tag{1.d}$$

where $\boldsymbol{A_i}$ and $\boldsymbol{A_e}$ are short notations for the internal and external radiation operators, respectively.

Notably, formulation (1) is certainly not the unique possible way to write down the scattering equations. A first possible alternative is the so-called CS-EB model [22], [23], i.e.:

$$\underline{W} = p\underline{E}_i + p\boldsymbol{A_{iMOD}}[\underline{W}] \tag{2.a}$$

$$\underline{E}_s = \boldsymbol{A_e}[\underline{W}] \tag{2.b}$$

where $\underline{W} = p\underline{E}$ is the so-called contrast source, $\boldsymbol{A_{iMOD}}[\underline{W}] = k_b^2\int_V \mathbf{G}(\underline{r}-\underline{r}')[\underline{W}(\underline{r}') - \underline{W}(\underline{r})]\,d\underline{r}'$, and p embeds the unknown characteristics of the object (see Table 1 for more details).

In case of vectorial problems (i.e., 3-D problems and 2-D problems under TE polarization) the so-called SPF model (see [24], [25]) can also be eventually used. According to this latter, formulation (1) can be recast as:

$$\underline{F} = \underline{E}_i + \boldsymbol{A_{iSPF}}[q\underline{F}] \tag{3.a}$$

$$\underline{E}_s = \boldsymbol{A_e}[q\underline{F}] \tag{3.b}$$

wherein q is the unknown function describing the electromagnetic parameters of the target, $\underline{F} = (1+\chi L)\underline{E}$, L being a constant depending on the shape of the considered exclusion volume (see [27] for more details); $\boldsymbol{A_{iSPF}} = P.V.k_b^2\int_V \mathbf{G}(\underline{r},\underline{r}')\,\chi(\underline{r}')\,\underline{E}(\underline{r}')\,d\underline{r}'$ by denoting with $P.V.\int(\cdot)$ a shape dependent principal value integral and being $q = \chi(1+\chi L)^{-1}$.

Note that the three models all present the same identical structure for the state equation.

When the solution of the inverse scattering problem starting from the EFIE is attempted, one has to face with the compactness of the radiation operator $\boldsymbol{A_e}$ (leading to ill-posedness) and the non-linearity arising from the fact that $\underline{E}$ (or, equivalently, $\underline{W}$) and χ are both unknowns. To counteract the aforementioned difficulties, several approximation strategies have been proposed that allow a linearization of the problem, by paying the price of a reduction of the class of profiles which can be considered.

As a first possibility, if (1.c) is formally inverted in the unknown $\underline{E}$ and the Neumann series is exploited in the arising equation, the *Born series* is derived [26]. Then, the first order *Born approximation* (BA) derives by considering the first term of the series. By so doing, the scattering problem becomes linear in the unknown χ (see Table 1) [26].

In the same way, by virtue of the identical structure of the inherent state equation, CS-EB and SPF *approximations* can be derived to linearize the problem in the auxiliary unknown p and q, respectively. Please refer to Table 1 for a summary of the arising linear approximations equations.

III. FOURIER ANALYSIS OF THE APPROXIMATED MODELS

In the field of tomography, a very important result is the *Fourier diffraction theorem* [28] which describes the existing relationship between the scattered field and the Fourier transform of the contrast function under the BA [26], [28].

In this paper, we take advantage from the above theory in two different ways. First, a Fourier analysis for CS-EB and SPF approximations (in the following referred as CS-EBA and SPFA) is derived. Then, the achieved results are used as a tool to design volumetric invisibility cloaks.

A. EXTENSION OF THE FOURIER DIFFRACTION THEOREM

The CS-EBA and SPFA are based on the definition of an auxiliary unknown, thereinafter named $\eta\left(\underline{r}\right)$, directly related to the original unknown $\chi\left(\underline{r}\right)$, see Table 1.

Then, when plane wave incident fields and far-field observations of the scattered field on a closed surface $\Gamma \notin V$ are considered, the data equation particularizes (as for the BA in [26] and [28]) as follows:

$$\underline{E}_s\left(\underline{r}\right) = \gamma\left(k_b\right)\int_V \eta\left(\underline{r}'\right) e^{-j\left(\underline{k}_i-\underline{k}_o\right)\cdot\underline{r}'} d\underline{r}', \quad \underline{r} \in \Gamma \quad (4.a)$$

$$\eta\left(\underline{r}\right) = \begin{cases} \chi\left(\underline{r}\right) & for\ BA \\ p\left(\underline{r}\right) & for\ CS-EBA \\ q\left(\underline{r}\right) & for\ SPFA \end{cases} \quad (4.b)$$

with $\underline{k}_o = \left(k_{ox}, k_{oy}, k_{oz}\right)$ and $\underline{k}_i = \left(k_{ix}, k_{iy}, k_{iz}\right)$ indicating the observation and incidence direction, respectively, and γ is a constant depending of frequency.

Note that in deriving (4.a) the asymptotic form of the Green's function and the approximation of the total field to the incident field have been considered.

It proves now useful to consider the expression of the Fourier transform of $\eta\left(\underline{r}\right)$, which (apart from an unessential constant) reads [29]:

$$\mathcal{FT}\left[\eta\left(\underline{r}\right)\right] = \tilde{\eta}\left(\underline{K}\right) = \int_V \eta(\underline{r}')e^{-j\underline{K}\cdot\underline{r}'} d\underline{r}' \quad (5)$$

where $\underline{K} = \left(K_x, K_y, K_z\right)$ is the set of spatial frequencies and $\mathcal{FT}[\cdot]$ indicates the Fourier transform operator. Then, by comparing (4.a) and (5), one immediately gets that the scattered field can be considered the restriction of $\tilde{\eta}$ to the sub-set of spatial frequencies Ω given by $\underline{K} = \left(\underline{k}_i - \underline{k}_o\right)$. In particular, for a complete set of illuminating plane waves with $\underline{k}_o$ varying over sphere of radius k_b, the region Ω will fill the volume of a sphere with radius $2k_b$ and centered at the origin of $\underline{K}$ space, the so called *Ewald limiting sphere* (ELS) [26]. This means that the knowledge of the scattered field for all incident-observation angles is equivalent to the knowledge of the low-pass version of the η function [30].

B. THE FOURIER DIFFRACTION THEOREM AS A WAY TO INVISIBILITY

The circumstances above can be conveniently used in case of invisibility problems. As a matter of fact, when an invisibility condition is looked for, the aim is to cancel out the scattered field from an object by covering it with a properly designed coat. Hence, a trivial condition for invisibility comes from the fact that if the spectral content $\tilde{\eta}$ of the overall scatterer (i.e., object plus cloak) is zero inside the ELS, the corresponding scattered field will be zero as well, and hence η can be considered invisible (see Fig.1 for a pictorial representation).

Quite interestingly, the condition depicted in Fig.1(c), for $\eta = \chi$, includes the results in [31] (which includes in turn the SC formula (10) in [1], particularized for the TM case) as special cases.

On the other side, as $\tilde{\eta}$ is the Fourier transform of a function having limited support, one will not be able to have a function $\tilde{\eta}$ which is exactly zero in a non-zero domain [29]. Hence, the actual condition which can be pursued has to be given in terms of the energy of the $\tilde{\eta}$ function in the ELS.

Then, by referring to the scenario depicted in Fig.2, the design problem becomes the synthesis of the electromagnetic parameters $\bar{\eta}_1 \in V_1$[1] of a coat enclosing the object to be hidden with known properties $\bar{\eta}_0 \in V_0$, in such a way to minimize the functional:

$$\psi\left(\bar{\eta}_1\right) = \left\|\widehat{\Pi}_\Omega \mathcal{FT}\left[\eta_0 + \eta_1\right]\right\|_\Omega^2 \quad (6)$$

in which $\widehat{\Pi}_\Omega$ is a mask function that is equal to 1 for all the spatial frequencies belonging to the ELS Ω, and zero elsewhere, while $\eta_0 = ZP\left[\bar{\eta}_0\right]$ and $\eta_1 = ZP\left[\bar{\eta}_1\right]$, with ZP indicating the zero-padding operation in the spatial domain.

Functional (6) is quadratic (and definite positive) in the unknown function $\bar{\eta}_1$, so that its minimization is relatively easy.

It is interesting to note that for all those frequencies where permittivities can be considered to be (approximately) con-

[1] V_1 is the domain arising from the difference between a larger domain with given dimensions and the domain V_0 occupied by the object to be hidden.

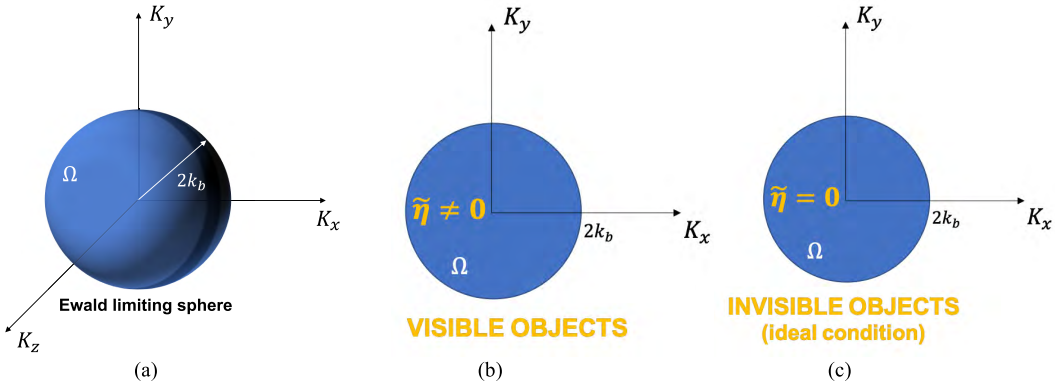

FIGURE 1. Pictorial representation of the extended diffraction theorem. Ewald limiting sphere (ELS) (a). 2-D slice of the ELS for visibility (b) and invisibility (c) condition.

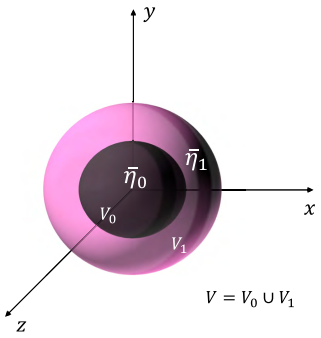

FIGURE 2. Sketch of the scenario dealt with in the invisibility problem.

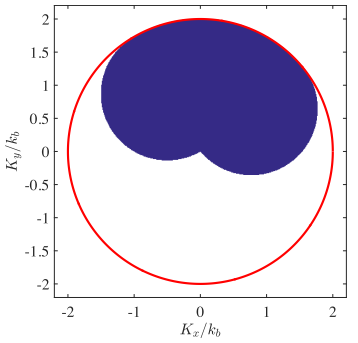

FIGURE 3. 2-D slice of the forbidden volume Ω (blue) for incident directions from 40° to 120°. The red line represents the ELS.

stant, successful optimization of (6) at the higher frequency of interest also implies invisibility at the lower frequencies.

More details on the implementation of the optimization procedure are deferred to the Appendix.

C. HANDLING DIFFERENT INVISIBILITY CONFIGURATIONS

When considering all possible incidence and observation directions, the knowledge of the scattered fields is equivalent to the knowledge of the spectral content of $\eta\left(\underline{r}\right)$ in the ELS. This means that whatever the direction of the incident field and the observation direction, a given object covered with the synthesized coat will result invisible as long as the correspondent spectral content is shifted outside the ELS (*multiview-multistatic* configuration).

However, *aspect limited* configurations could also be of interest. It is interesting to note that in such a case the proposed approach can still be applied provided the shape of the volume Ω is properly modified. In particular, to deal with different illumination configurations, the following equation:

$$\left|\underline{K} - \underline{k}_i\right|^2 = k_b^2 \tag{7}$$

can be used as a design equation that allows to define new sets of forbidden region Ω by varying the span of $\underline{k}_i$ in limited angular sectors. In Fig. 3 is depicted an example of spectral coverage in case of *aspect limited* illumination. In this case, by shifting out the energy from the blue region, the invisibility could be reached for all plane waves with an incidence angle in the range 40° to 120° (and for all the observation directions).

A typical *aspect limited* scenario occurs when the object to be hidden is located in a medium different from the free-space and/or it can be illuminated by one side only (e.g., subsurface scenario). In this case, the role of the measurement configuration as well as the effect of the antennas' radiation characteristics on the spectral coverage has been extensively studied in literature and the corresponding relevant set of spatial frequencies have been derived under the BA [32]–[35]. Interestingly, these results can be profitably used for our invisibility scope. In fact, the minimization of functional (6) can still be carried out as long as the new set of spatial frequencies is considered as forbidden region Ω for the spectral coverage. In this case, we deal with a *RX-invisibility*, in the sense that a reduction in the scattered field is reached on the region directly illuminated by the incident fields, while no control can be carried out beyond the object.

Last but not least, let us note that by proper expansions into plane waves, the approach also can be profitably used in case of sources and receivers not located in the far field of the scatterer (provided reactive fields can be neglected).

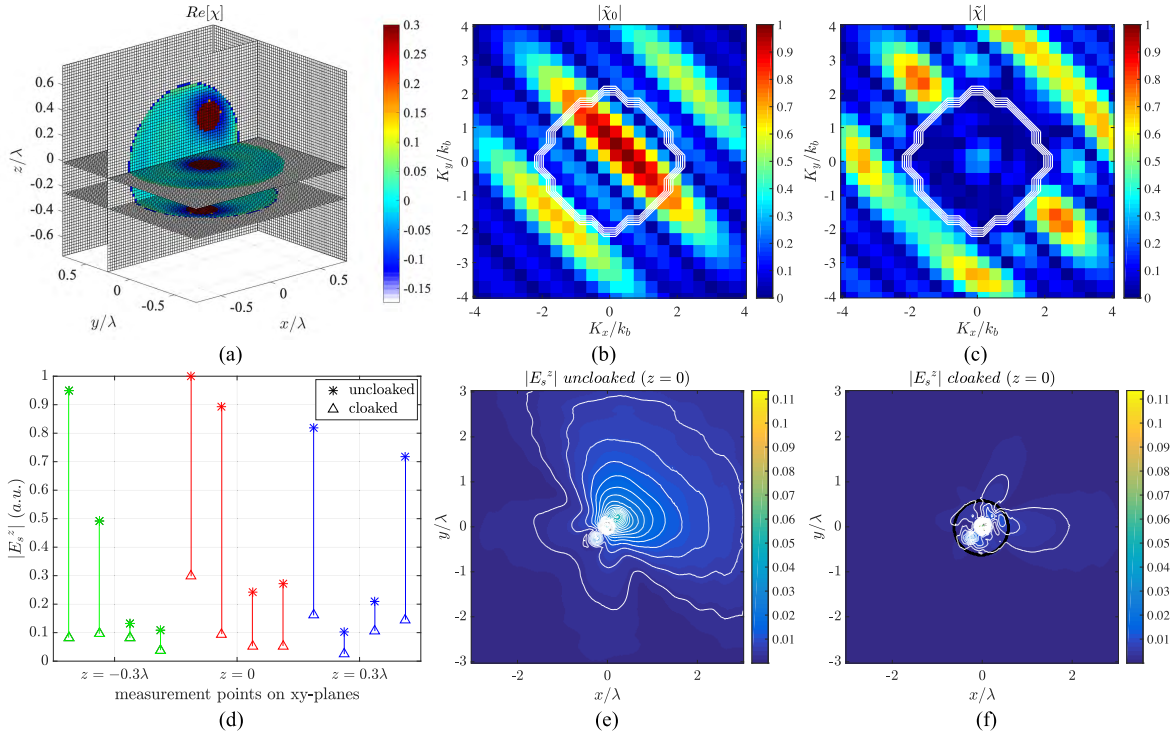

FIGURE 4. Three spheres target in BA. Real part of the contrast function of the cloaking device (a). Fourier transform of χ_0 (b) and χ (c) function. The white line indicates the contour of the Ewald sphere. Amplitude of the z-component of the scattered field at different observation points (d) and on domain for the uncloaked (e) and cloaked (f) target. In (e)-(f) the black lines represent the target contour, while the white lines are the contour levels of the scattered field.

IV. NUMERICAL ANALYSIS

The assessment of the design approach is carried out for 3-D objects. In the following, two scenarios are considered to deal with the BA and SPFA case, respectively.

The first target consists of three identical spheres with radius 0.12λ and $\varepsilon_s = 2$ located at $(-0.25, -0.25, -0.25)\lambda$, (0,0,0) and (0.25,0.25,0.25)λ, respectively, while the coat region V_1 results from the intersection between a bigger sphere with radius 0.6λ and the volume V_0 occupied by the target. By considering as forbidden domain Ω the entire ELS, the minimization problem (6) is solved in the BA (so, $\eta \equiv \chi$) to determine the contrast value $\bar{\chi}_1 \in V_1$. The resulting profile is shown in Fig.4(a) and it has been achieved after just 7 iterations of the optimization algorithm in 6.5 seconds on a laptop with 1.3GHz Intel Core i7 and 16GB RAM. In Fig. 4(b) and 4(c) the Fourier transform of the contrast function pertaining to the uncloaked and cloaked object is depicted, respectively. As it can be seen, the initial spectral content inside the ELS is shifted outside the ELS, so that the energy content of $\tilde{\eta}$ corresponding to actually scattered fields is considerably reduced. To check the functionality of the device, a forward scattering problem is solved through a full wave simulation for a TM incident plane wave ($\underline{E}_i = E_i^z \hat{z}$) travelling from ($\theta = 90°, \phi = 0°$), θ and ϕ being the elevation and azimuth angles, respectively. As it can be observed from the slice plot in Figs.4(e) and 4(f) at $z = 0$ (as well as in all other slices) the scattered field is considerably reduced outside the cloaking region. The impact of such a reduction can be also appraised from Fig. 4(d), in which the scattered field is evaluated on $N_m = 12$ observation points equally spaced on 3 closed circumferences located at $R_m = 2.88\lambda$ on the three planes $z = -0.3\lambda$, $z = 0$ and $z = 0.3\lambda$, respectively, and with an angular shift of 30° amongst measurements at the different planes.

Finally, the figure of merit (*FoM*) introduced in [4] has been evaluated to better appraise the cloaking effect. In particular, it refers to the ratio between the scattering cross-section (SCS) of the covered and bare object. By following [19], for each illumination direction the SCS is defined as:

$$SCS\left(\underline{r}_t\right) = 4\pi R_m^2 \left[\frac{1}{N_m}\sum_{m=1}^{N_m}\frac{\left|\underline{E}_s\left(\underline{r}_m, \underline{r}_t\right)\right|^2}{\left|\underline{E}_i\left(\underline{r}_m, \underline{r}_t\right)\right|^2}\right] \tag{8.a}$$

wherein $\underline{r}_t, \underline{r}_m$ indicate the transmitters and receivers locations.

Then:

$$FoM = \frac{SCS^{cloaked}}{SCS^{uncloaked}} \tag{8.b}$$

As such, the *FoM* leads to less-than-unity values (thus a negative sign in dB unit) if the scattering of the bare object is stronger with respect to the cloaked object.

For the example at hand, $FoM = -13.68dB$.

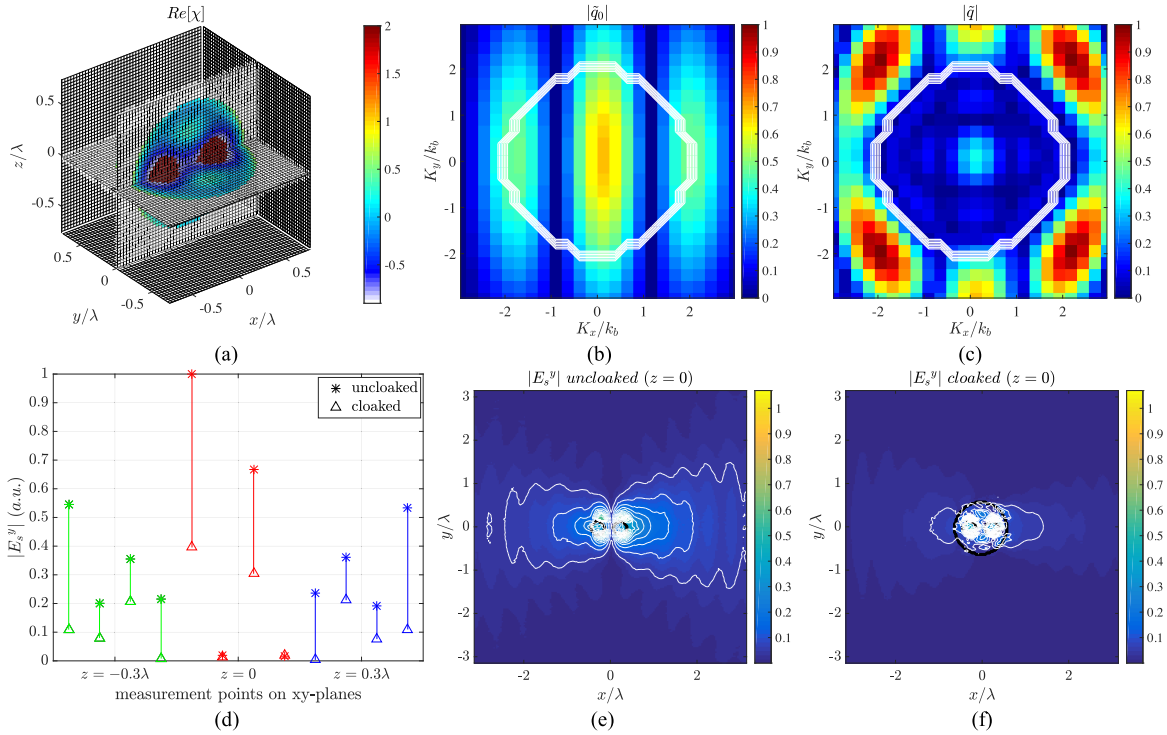

FIGURE 5. Two spheres target in SPFA. Real part of the contrast function of the cloaking device (a). Fourier transform of q_0 (b) and q (c) function. The white line indicates the contour of the Ewald sphere. Amplitude of the y-component of the scattered field at different observation points (d) and on domain for the uncloaked (e) and cloaked (f) target. In (e)-(f) the black lines represent the target contour, while the white lines are the contour levels of the scattered field.

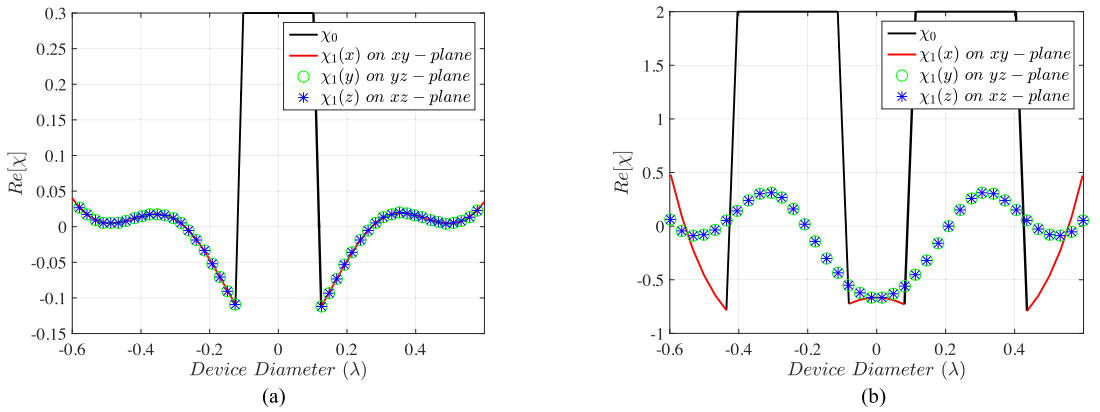

FIGURE 6. Cuts of the real part of the overall contrast function for the example within BA (a) and SPFA (b). The black line is relative to the bare object, while the red line, and the green and blue markers represent the 1-D cut of the synthesized contrast function along x ($y = z = 0$), y ($x = z = 0$) and z ($x = y = 0$) axis, respectively.

The second example deals with two identical spheres with radius 0.15λ, $\varepsilon_s = 3$, located at $(-0.2585,0.2583,0)\lambda$ and $(0.2585,0.2583,0)\lambda$, respectively. As we deal with scatterers whose permittivity is larger, thus possibly inhibiting the use of the BA, the invisibility cloak design is now performed through the SPFA. In particular, we look for a coat whose external radius is 0.6λ.

Accordingly, the initial contrast function $\chi_0(\underline{r})$ of the bare target is converted into the auxiliary variable $q_0(\underline{r})$ by following formulas in Table 1 ($L = 1/3$)[2]. Then, the optimization problem is solved in the unknown $\eta_1 = q_1$, which is finally converted into χ_1 to make up the cloaking device $\chi = \chi_0 + \chi_1$, see Fig. 5(a). The spectral content of the q_0 and q function is shown in Fig. 5(b) and 5(c), respectively, from which the shifting of the energy content outside the ELS can be appraised. The scattered field is calculated through full

[2]This allows to halve the maximum value of the target's permittivity.

wave simulations of the two targets (bare and covered). In this case, a TE plane wave from ($\theta = 90°, \phi = 0°$), has been considered as incident field ($\underline{E}_i = E_i^y \hat{y}$). From Figs. 5(d)-(f) the reduction of the scattering effect can be appraised from both a qualitative (scattered field on domain) and quantitative (scattered field on observation points, which are the same of the previous example) point of view. Finally, for this example, the value of the *FoM* results as $-8.1dB$.

In order to get a more quantitative understanding of the final cloak, in Fig. 6 we report 1-D cuts of the constitutive parameters of the designed coats, for both the BA (Fig. 6(a)) and SPFA (Fig. 6(b)) based examples. In particular, for each plane the corresponding central cut of the contrast function is reported.

V. CONCLUSIONS

The design of (volumetric) invisibility cloaks has been faced within the framework of inverse scattering problems. In particular, provided one amongst different linear approximations holds true, simple Fourier analysis can be applied, and one can design the cloak by shifting the spectral content of the unknown outside the visible range. In fact, on the basis of the results in Section III.A this corresponds to scattered fields as small as possible. From a physical point of view, the spectral shift of the unknown function can be conceived as way to deal with non-radiating contrast sources.

A feasibility study of the proposed method has been successfully carried out. In the literature, no approach based on inverse scattering theory and tools (but for [15]–[20]) seems to exist. The proposed approach exhibits some similarities with the SC technique [1] as both of them (opposite to TO) mean to design 'ad hoc' cloaks, and just exploit isotropic materials. Also, both of them only can work if some hypotheses on the object to be hidden holds true. On the other side, even if one still cannot apply it to Perfect Electric Conductors (PEC) or 'large' objects, the proposed approach outperforms the SC technique both in terms of its range of applicability as well as in its capability to deal with non-canonical objects. Last, but not least, the proposed approach can be easily adapted to the quest for different kind of 'partial' invisibility (see Section III.C).

Notably, actual realization of the designed cloaks requires to rely on some homogenization techniques [36]. As a suitable alternative, constraints may be eventually enforced on the quantity at hand in (6) such as, for example, step wise constant behavior, or physical feasibility within given bounds. Enforcing a smoothly varying profile for the cloak can also be of interest in order to facilitate homogenization, as exploited in [15] for antennas design.

APPENDIX

The minimization of functional (6) is carried out through a conjugate gradient least square algorithm. To this aim, the gradient of (6) and a direction of descent must be derived.

To this end, let us consider a variation of ψ due to an increment $\Delta\eta_1$:

$$\begin{aligned}\Delta\psi_{\eta_1} &= \left\langle \widehat{\Pi}_\Omega \mathcal{FT}\left(\eta_0+\eta_1\right), \widehat{\Pi}_\Omega \mathcal{FT}\left(\Delta\eta_1\right)\right\rangle + c.c. \\ &= \left\langle \mathcal{FT}^{-1}\left[\widehat{ZP}\widehat{\Pi}_\Omega \mathcal{FT}\left(\eta_0+\eta_1\right)\right], \Delta\eta_1\right\rangle + c.c. \\ &= \left\langle \Pi_{V_1}\mathcal{FT}^{-1}\left[\widehat{ZP}\widehat{\Pi}_\Omega \mathcal{FT}\left(\eta_0+\eta_1\right)\right], \Delta\bar{\eta}_1\right\rangle + c.c.\end{aligned} \tag{A.1}$$

wherein $\widehat{ZP}$ indicates a zero-padding operation in the frequency domain, Π_{V_1} is a mask function that is equal to 1 for all points belonging to V_1 and zero elsewhere, while $c.c.$ denotes the complex conjugation operation.

From (A.1) follows that the gradient of ψ with respect to the unknown is:

$$\nabla\psi_{\eta_1} = 2\Pi_{V_1}\mathcal{FT}^{-1}\left[\widehat{ZP}\Pi_\Omega \mathcal{FT}\left(\eta_0+\eta_1\right)\right] \tag{A.2}$$

Then, the update step λ is found such that minimizes the functional:

$$\Lambda(\lambda) = \psi\left(\bar{\eta}_1 + \lambda\Delta\bar{\eta}_1\right) = a\lambda^2 + b\lambda + c \tag{A.3}$$

whose minimum is given by $-\frac{b}{2a}$, with:

$$\begin{aligned} a &= \left\| \widehat{\Pi}_\Omega \mathcal{FT}\left(\Delta\eta_1\right)\right\|^2 \\ b &= 2Re\left\langle \widehat{\Pi}_\Omega \mathcal{FT}\left(\Delta\eta_1\right), \widehat{\Pi}_\Omega \mathcal{FT}\left(\eta_0+\eta_1\right)\right\rangle \\ c &= \left\| \widehat{\Pi}_\Omega \mathcal{FT}\left(\eta_0+\eta_1\right)\right\|^2 \end{aligned} \tag{A.4}$$

and where $\Delta\bar{\eta}_1$ is the update direction as defined from the conjugate gradient procedure at hand [37].

REFERENCES

[1] A. Alù and N. Engheta, "Achieving transparency with plasmonic and metamaterial coatings," *Phys. Rev. E, Stat. Phys. Plasmas Fluids Relat. Interdiscip. Top.*, vol. 2, no. 1, Jul. 2005, Art. no. 019906.
[2] A. Alù and N. Engheta, "Theory and potentials of multi-layered plasmonic covers for multi-frequency cloaking," *New J. Phys.*, vol. 10, no. 11, Nov. 2008, Art. no. 115036.
[3] A. Alù and N. Engheta, "Multifrequency optical invisibility cloak with layered plasmonic shells," *Phys. Rev. Lett.*, vol. 100, no. 11, Mar. 2008, Art. no. 113901.
[4] F. Bilotti, S. Tricarico, and L. Vegni, "Electromagnetic cloaking devices for TE and TM polarizations," *New J. Phys.*, vol. 10, no. 11, Nov. 2008, Art. no. 115035.
[5] A. Alù and N. Engheta, "Cloaking a Sensor," *Phys. Rev. Lett.*, vol. 102, no. 23, Jun. 2009, Art. no. 233901.
[6] S. Tricarico, F. Bilotti, A. Alù, and L. Vegni, "Plasmonic cloaking for irregular objects with anisotropic scattering properties," *Phys. Rev. E, Stat. Phys. Plasmas Fluids Relat. Interdiscip. Top.*, vol. 81, no. 2, Feb. 2010, Art. no. 026602.
[7] A. Monti, F. Bilotti, and A. Toscano, "Optical cloaking of cylindrical objects by using covers made of core-shell nanoparticles," *Opt. Lett.*, vol. 36, no. 23, pp. 4479–4481, 2011.
[8] M. Fruhnert *et al.*, "Tunable scattering cancellation cloak with plasmonic ellipsoids in the visible," *Phys. Rev. B, Condens. Matter*, vol. 93, no. 24, Jun. 2016, Art. no. 245127.
[9] J. B. Pendry, D. Schurig, and D. R. Smith, "Controlling electromagnetic fields," *Science*, vol. 312, pp. 1780–1782, Jun. 2006.
[10] G. Castaldi, I. Gallina, and V. Galdi, "Nearly perfect nonmagnetic invisibility cloaking: Analytic solutions and parametric studies," *Phys. Rev. B, Condens. Matter*, vol. 80, no. 12, Sep. 2009, Art. no. 125116.
[11] G. Castaldi, I. Gallina, V. Galdi, A. Alù, and N. Engheta, "Power scattering and absorption mediated by cloak/anti-cloak interactions: A transformation-optics route toward invisible sensors," *J. Opt. Soc. Amer. B*, vol. 27, no. 10, pp. 2132–2140, 2010.

[12] W. Tang, C. Argyropoulos, E. Kallos, W. Song, and Y. Hao, "Discrete coordinate transformation for designing all-dielectric flat antennas," *IEEE Trans. Antennas Propag.*, vol. 58, no. 12, pp. 3795–3804, Dec. 2010.
[13] C. Mateo-Segura, A. Dyke, H. Dyke, S. Haq, and Y. Hao, "Flat Luneburg lens via transformation optics for directive antenna applications," *IEEE Trans. Antennas Propag.*, vol. 62, no. 4, pp. 1945–1953, Apr. 2014.
[14] O. M. Bucci, I. Catapano, L. Crocco, and T. Isernia, "Synthesis of new variable dielectric profile antennas via inverse scattering techniques: A feasibility study," *IEEE Trans. Antennas Propag.*, vol. 53, no. 4, pp. 1287–1297, Apr. 2005.
[15] R. Palmeri, M. T. Bevacqua, A. F. Morabito, and T. Isernia, "Design of artificial-material-based antennas using inverse scattering techniques," *IEEE Trans. Antennas Propag.*, vol. 66, no. 12, pp. 7076–7090, Dec. 2018.
[16] T. Isernia, R. Palmeri, A. F. Morabito, and L. D. Donato, "Inverse scattering and compressive sensing as e.m. design tool," in *Proc. IEEE AP-S Symp. Antennas Propag. USNC/URSI Nat. Radio Sci. Meeting*, Jul. 2017, pp. 433–434.
[17] R. Palmeri, A. F. Morabito, and T. Isernia, "Design of a varying dielectric profile antenna generating reconfigurable $\Sigma - \Delta$ pattern via inverse scattering techniques," in *Proc. Int. Conf. Electromagn. Adv. Appl. (ICEAA)*, Aug. 2017, pp. 258–265.
[18] R. Palmeri, M. T. Bevacqua, A. F. Morabito, and T. Isernia, "A modified contrast source inversion method for the synthesis of innovative dielectric devices," in *Proc. 12th Eur. Conf. Antennas Propag.*, 2018, pp. 1–4.
[19] L. Di Donato, T. Isernia, G. Labate, and L. Matekovits, "Towards printable natural dielectric cloaks via inverse scattering techniques," *Sci. Rep.*, vol. 7, no. 1, p. 3680, Jun. 2017.
[20] L. Di Donato, L. Crocco, M. T. Bevacqua, and T. Isernia, "Quasi-invisibility via inverse scattering techniques," in *Proc. IEEE Conf. Antenna Meas. Appl.*, Nov. 2014, pp. 1–2.
[21] M. Bertero and P. Boccacci, *Introduction to Inverse Problems in Imaging*. Boca Raton, FL, USA: CRC Press, 1998.
[22] T. Isernia, L. Crocco, and M. D'Urso, "New tools and series for forward and inverse scattering problems in lossy media," *IEEE Geosci. Remote Sens. Lett.*, vol. 1, no. 4, pp. 327–331, Oct. 2004.
[23] M. D'Urso, I. Catapano, L. Crocco, and T. Isernia, "Effective solution of 3-D scattering problems via series expansions: Applicability and a new hybrid scheme," *IEEE Trans. Geosci. Remote Sens.*, vol. 45, no. 3, pp. 639–648, Mar. 2007.
[24] L. Tsang and J. Kong, "Scattering of electromagnetic waves from random media with strong permittivity fluctuations," *Radio Sci.*, vol. 16, no. 3, pp. 303–320, Jun. 1981.
[25] J. Ma, W. C. Chew, C.-C. Lu, and J. Song, "Image reconstruction from TE scattering data using equation of strong permittivity fluctuation," *IEEE Trans. Antennas Propag.*, vol. 48, no. 6, pp. 860–867, Jun. 2000.
[26] A. J. Devaney, *Mathematical Foundations of Imaging, Tomography and Wavefield Inversion*. Cambridge, U.K.: Cambridge Univ. Press, 2012.
[27] W. C. Chew, *Waves and Field in Inhomogeneous Media*. New York, NY, USA: IEEE Press, 1995.
[28] A. C. Kak, and M. Slaney, *Principles of Computerized Tomographic Imaging*. New York, NY, USA: IEEE Press, 1988 pp. 203–274.
[29] E. W. Hansen, *Fourier Transforms: Principles and Applications*. Hoboken, NJ, USA: Wiley, 2014.
[30] R. Palmeri and T. Isernia, "A simple approach to invisibility under different linear approximations," in *Proc. 2nd URSI Atlantic Radio Sci. Meeting*, Sep. 2018, pp. 368–385.
[31] G. Labate and L. Matekovits, "Invisibility and cloaking structures as weak or strong solutions of devaney-wolf theorem," *Opt. Express*, vol. 24, no. 17, pp. 19245–19253, 2016.
[32] G. Leone and F. Soldovieri, "Analysis of the distorted born approximation for subsurface reconstruction: Truncation and uncertainties effects," *IEEE Trans. Geosci. Remote Sens.*, vol. 41, no. 1, pp. 66–74, Jan. 2003.
[33] R. Persico, R. Bernini, and F. Soldovieri, "The role of the measurement configuration in inverse scattering from buried objects under the Born approximation," *IEEE Trans. Antennas Propag.*, vol. 53, no. 6, pp. 1875–1887, Jun. 2005.
[34] F. Soldovieri, R. Persico, and G. Leone, "Effect of source and receiver radiation characteristics in subsurface prospecting within the distorted Born approximation," *Radio Sci.*, vol. 40, no. 3, pp. 1–13, Jun. 2005.
[35] R. Persico, F. Soldovieri, and G. Leone, "A microwave tomographic imaging approach for multibistatic configuration: The choice of the frequency step," *IEEE Trans. Instrum. Meas.*, vol. 55, no. 6, pp. 1926–1934, Dec. 2006.
[36] S. Datta, C. T. Chan, K. M. Ho, and C. M. Soukoulis, "Effective dielectric constant of periodic composite structures," *Phys. Rev. B, Condens. Matter*, vol. 48, no. 20, p. 14936, 1993.
[37] A. Bjork, *Numerical Methods for Least Square Problems*, vol. 51. Philadelphia, PA, USA: SIAM, 1996.

ROBERTA PALMERI was born in Catania, Italy, in 1989. She received the M.S. Laurea degree *(summa cum laude)* in telecommunication engineering from the University of Catania, Catania, Italy, in 2014, and the Ph.D. degree in information engineering from the Università degli Studi Mediterranea di Reggio Calabria, Reggio Calabria, Italy, in 2018, where she is currently a Research Fellow of the LEMMA Research Group. Her scientific activities are concerned with inverse problems in electromagnetics. In particular, she is presently focused on the development of new strategies based on inverse scattering for the synthesis of innovative devices. She was a recipient of the Best Italian Remote Sensing Thesis Prize from the IEEE Geoscience and Remote Sensing South Italy Chapter, in 2014, the IEEE Antennas and Propagation Society (Central and South Italy Chapter) Prize, in 2017, and the Young Scientist Award at the 2nd URSI Atlantic Radio Science Meeting, in 2018.

TOMMASO ISERNIA received the Laurea *(summa cum laude)* and Ph.D. degrees from the University of Naples Federico II, Naples, Italy.

He is currently a Full Professor of electromagnetic fields with the Università degli Studi Mediterranea di Reggio Calabria, Reggio Calabria, Italy, where he is the DIIES department director and supervises the LEMMA Research Group and the Ph.D. course in information engineering. He is also with the Consorzio Nazionale Italiano per le Telecomunicazioni Consortium, where he serves as a Member of the Board of Administrators. He is also involved in the field synthesis problems for biomedical imaging and therapeutic applications. His current research interests include inverse problems in electromagnetics, particularly, emphasis on phase retrieval, inverse scattering, and antenna synthesis problems. He was a recipient of the G. Barzilai Award from the Italian Electromagnetics Society, in 1994.